DOE F 241.3
(2-01) p.1 of 2

UNITED STATES DEPARTMENT OF ENERGY (DOE)
Announcement of Scientific and Technical Information (STI)
(For Use By Financial Assistance Recipients and Non-M&O/M&I Contractors)

OMB CONTROL NO. 1910-1400

PART I: STI PRODUCT DESCRIPTION
(To be completed by Recipient/Contractor)

A. STI Product Identifiers

1. REPORT/PRODUCT NUMBER(s)
None

2. DOE AWARD/CONTRACT NUMBER(s)
DE-FC36-97ID13554

3. OTHER IDENTIFYING NUMBER(s)
None

B. Recipient/Contractor

University of Alabama, Metallurgical and Materials Engineering Department, Tuscaloosa, Alabama, 35487-0202

C. STI Product Title

Enhanced Inclusion Removal from Steel in the Tundish

D. Author(s)

R. C. Bradt
M.A.R. Sharif

E-mail Address(es):
rcbradt@coe.eng.ua.edu

E. STI Product Issue Date/Date of Publication

09 (MM) 25 (DD) 2009 (YYYY)

F. STI Product Type (*Select only one*)

☒ 1. TECHNICAL REPORT
☒ *Final* ☐ *Other (specify)* _____

☐ 2. CONFERENCE PAPER/PROCEEDINGS

Conference Information (title, location, dates)

☐ 3. JOURNAL ARTICLE
a. TYPE: ☐ *Announcement Citation Only* ☐ *Preprint* ☐ *Postprint*
b. JOURNAL NAME
c. VOLUME _____ *d. ISSUE* _____
e. SERIAL IDENTIFIER (e.g. ISSN or CODEN)

☐ 4. OTHER, SPECIFY

G. STI Product Reporting Period

05 (MM) 17 (DD) 1998 (YYYY) Thru 12 (MM) 31 (DD) 2008 (YYYY)

H. Sponsoring DOE Program Office

Office of Industrial Technologies (OIT)(EE20)

I. Subject Categories *(list primary one first)*

32 Energy Conservation, Consumption and Utilization
Keywords: Steel Tundish, Inclusions

J. Description/Abstract

The objective of this project was to develop an effective chemical filtering system for significantly reducing the content of inclusion particles in the steel melts exiting the tundish for continuous casting. This project combined a multi-process approach that aimed to make significant progress towards an "inclusion-free" steel by incorporating several interdependent concepts to reduce the content of inclusions in the molten steel exiting the tundish for the caster. The goal is to produce "cleaner" steel.

K. Intellectual Property/Distribution Limitations
(must select at least one; if uncertain contact your Contracting Officer (CO))

☒ 1. UNLIMITED ANNOUNCEMENT *(available to U.S. and non-U.S. public; the Government assumes no liability for disclosure of such data)*

☐ 2. COPYRIGHTED MATERIAL: *Are there any restrictions based on copyright?* ☐ *Yes* ☐ *No.*
If yes, list the restrictions as contained in your award document

☐ 3. PATENTABLE MATERIAL: THERE IS PATENTABLE MATERIAL IN THE DOCUMENT.
INENTION DISCLOSURE SUBMITTED TO DOE:
DOE Docket Number: S-
(Sections are marked as restricted distribution pursuant to 35 USC 205)

☐ 4. PROTECTED DATA: ☐ CRADA ☐ *Other, specify*
Release date (required) no more than 5 years from date listed in Part I.E. above ___ (MM) ___ (DD) ____ (YYYY)

☐ 5. SMALL BUSINESS INNOVATION RESEARCH (SBIR) DATA
Release date (required) no more than 4 years from date listed in Part I.E. above ___ (MM) ___ (DD) ____ (YYYY)

☐ 6. SMALL BUSINESS TECHNOLOGY TRANSFER RESEARCH (STTR) DATA
Release date (required) no more than 4 years from date listed in Part I.E. above ___ (MM) ___ (DD) ____ (YYYY)

☐ 7. OFFICE OF NUCLEAR ENERGY APPLICED TECHNOLOGY

L. Recipient/Contract Point of Contact *Contact for additional information (contact or organization name To be included in published citations and who would Receive any external questions about the content of the STI Product or the research contained herein)*

Dr. R. C. Bradt
Name and/or Position
rcbradt@eng.ua.edu (205)348-0663
E-mail *Phone*
Metallurgical and Materials Engineering Department, University of Alabama, Tuscaloosa, AL

UNITED STATES DEPARTMENT OF ENERGY (DOE)
Announcement of Scientific and Technical Information (STI)
(For Use By Financial Assistance Recipients and Non-M&O/M&I Contractors)

OMB CONTROL NO.
1910-1400

PART II: STI PRODUCT MEDIA/FORMAT and LOCATION/TRANSMISSION

(To be completed by Recipient/Contractor)

A. Media/Format Information:

1. MEDIUM OF STI PRODUCT IS:
   ☒ Electronic Document ☐ Computer Medium
   ☐ Audiovisual Material ☐ Paper ☐ No Full-text
2. SIZE OF STI PRODUCT 38 Pages, 1,264 KB
3. SPECIFY FILE FORMAT OF ELECTRONIC DOCUMENT BEING TRANSMITTED, INDICATE:
   ☐ SGML ☐ HTML ☐ XML ☒ PDF Normal
   ☐ PDF Image ☐ TIFFG4
   ☐ WP-indicate Version (*5.0 or greater)* _____
   Platform/operation system _____
   ☐ MS-indicate Version (*5.0 or greater)* _____
   Platform/operation system _____
   ☐ Postscript _____
4. IF COMPUTER MEDIUM OR AUDIOVISUAL MATERIAL:
   a. Quantity/type (*specify)* _____
   b. Machine compatibility (*specify)* _____
   c. Other information about product format a user needs to know:
   _____

B. Transmission Information:

1. STI PRODUCT IS BEING TRANSMITTED:
   ☒ a. Electronically via E-Link
   b. Via mail or shipment to address indicated in award document (*Paper product, CD-ROM, diskettes, video cassettes, etc.)*
   _____
2. INFORMATION PRODUCT FILE NAME
   ☒ *(of transmitted electronic format)*
   TRP9757NonPropFinalReport

PART III: STI PRODUCT REVIEW/RELEASE INFORMATION

(To be completed by DOE)

A. STI Product Reporting Requirements Review.

☐ 1. THIS DELIVERABLE COMPLETES ALL REQUIRED DELIVERABLES FOR THIS AWARD
☐ 2. THIS DELIVERABLE FULFILLS A TECHNICAL INFORMATION REPORTING REQUIREMENT, BUT SHOULD NOT BE DISSEMINATED BEYOND DOE.

B. Award Office Is the Source of STI Product Availability

☐ THE STI PRODUCT IS NOT AVAILABLE IN AN ELECTRONIC MEDIUM. THE AWARDING OFFICE WILL SERVE AS THE INTERIM SOURCE OF AVAILABILITY.

C. DOE Releasing Official

☐ 1. I VERIFY THAT ALL NECESSARY REVIEWS HAVE BEEN COMPLETED AS DESCRIBED IN DOE G 241.1-1A, PART II, SECTION 3.0 AND THAT THE STI PRODUCT SHOULD BE RELEASED IN ACCORDANCE WITH THE INTELLECTUAL PROPERTY/DISTRIBUTION LIMITATION ABOVE.

Release by (*name)* _____

Date ___ ___ _____
MM DD YYYY

E-Mail _____

Phone _____

REPORT DOCUMENTATION PAGE

Title and Subtitle:

AISI/DOE Technology Roadmap Program for the Steel Industry
TRP 9757: Enhanced Inclusion Removal from Steel in the Tundish

Authors:

R.C. Bradt
M.A.R. Sharif

Performing Organization

University of Alabama
Metallurgical and Materials Engineering Department
Tuscaloosa, Alabama 35487-0202

Abstract

The objective of this project was to develop an effective chemical filtering system for significantly reducing the content of inclusion particles in the steel melts exiting the tundish for continuous casting. This project combined a multi-process approach that aimed to make significant progress towards an "inclusion-free" steel by incorporating several interdependent concepts to reduce the content of inclusions in the molten steel exiting the tundish for the caster. The goal is to produce "cleaner" steel.

Conventional mechanical trapping approach to the filtering process will result in the rapid clogging or plugging of the filter pores, purely as a consequence of the volume of inclusions contained in multiple ladles of steel. The innovative "filter system" being investigated in this research relied on physical and chemical phenomena that have been documented to occur in the tundish, specifically at the exit submerged entry nozzle (SEN). This filtering technique will exploit the intense mixing and recirculation of the melt via induced turbulence in artificially designed "roughened" zigzag or corrugated tundish baffle channels. This will increase the kinetics of agglomeration/coagulation processes of the inclusions within the melt to form larger inclusion particles that are easier to remove from the steel. The "designed" turbulence will also bring the molten steel stream along with the inclusion particles into frequent direct contact with the zigzag channel surfaces. The objective being that the inclusion particles will contact, then bond or adhere to the baffle channel surfaces. The filter channel surfaces will be made of $MgAl_2O_4$ spinel, a compound that is known to be of the surface chemical character that the inclusions will adhere to it. The $MgAl_2O_4$ spinel is one of the materials detected to be present in significant amounts in the accretions of clogged SEN's.

DOCUMENT AVAILABILITY

Reports are available free via the U.S. Department of Energy (DOE) Information Bridge:

Website: http://www.osti.gov/bridge

Reports are available to DOE employees, DOE contractors, Energy Technology Data Exchange (ETDE) representatives, and Informational Nuclear Information System (INIS) representatives from the following source:

Office of Scientific and Technical Information
P.O. Box 62
Oak Ridge, TN 37831
Tel: (865) 576-8401
Fax: (865) 576-5728
E-mail: reports@osti.gov
Website: http://www.osti.gov/contract.html

Acknowledgement: "This report is based upon work supported by the U.S. Department of Energy under Cooperative Agreement No. DE-FC36-97ID13554."

Enhanced Inclusion Removal from Steel in the Tundish

Final Project Report

May 2010

Prepared by

R. C. Bradt

Metallurgical and Materials Engineering Department

and

M. A. R. Sharif

Aerospace Engineering and Mechanics Department

The University of Alabama

Submitted to

American Iron and Steel Institute

American Iron and Steel Institute

Technology Roadmap Program

FINAL PROJECT REPORT

Title: **Enhanced Inclusion Removal from Steel in the Tundish** (TRP # 9757)

Project Period: May 17, 1998 to December 31, 2008

Date of Report: May 1, 2010

Recipient: The University of Alabama
Metallurgical and Materials Engineering Department
Tuscaloosa, Alabama 35487-0202

Contact(s): R.C. Bradt (205-348-0663, rcbradt@eng.ua.edu)
Metallurgical and Materials Engineering Department
The University of Alabama, Tuscaloosa, AL 35487-0202

M.A.R. Sharif (205-348-8052, msharif@eng.ua.edu)
Aerospace Engineering and Mechanics Department
The University of Alabama, Tuscaloosa, AL 35487-0280

Award Number: DE-FC36-97ID13554

Other Partners: Timken Company

TABLE OF CONTENTS

LIST OF FIGURES

LIST OF TABLES

EXECUTIVE SUMMARY

The objective of this research project was to eliminate inclusions from steel produced by the continuous casting process. The technical engineering route to achieve this goal was to apply phenomena that are already known to exist and occur in the tundish/caster portions of the continuous casting process. It is based on the formation of "inclusion based" accretions which develop and block the flow of the molten steel through the bottom of the submerged entry nozzle (SEN) which directs the molten steel into the caster. The approach is to relocate those accretions.

Formation of these accretions is a consequence of the thermo-chemistry of the steel making process and interactions with the refractories containing the molten steel. These accretions occur in the bottom of the SEN because (i) the surface chemistry of the SEN enables the accretions to nucleate and then "grow" and (ii) the turbulence generated by the flowing molten metal at the bottom of the SEN as it exits the nozzle and enters the caster. These accretions are not known to form any where else in the steelmaking process. This research is based on the premise that it is a combination of the chemistry and molten metal turbulence which causes these accretions to form in the SEN exit region.

In essence, the accretions form in the SEN from the alumina and spinel inclusions that are present in the molten steel. They nucleate the accretion mass and then contribute to its further growth by additional inclusions impacting and sticking to the original accretion nucleus from the turbulence at the SEN exit. As the accretions grow from more and more inclusions sticking, their size eventually blocks off the flow of the steel and inhibits the flow of steel from the tundish through the SEN to the caster. To prevent this process from occurring, this research endeavored to move the location of the accretion formation from the SEN to back upstream in the tundish itself. This would have two major benefits: (i) removal of inclusions from the steel, and (ii) preventing the blockage of the flow of inclusion containing molten steel through the SEN into the caster.

The methodology employed in this research was to recreate the accretion forming conditions within the tundish itself and therefore to remove the inclusions from the steel before they have any opportunity to enter the SEN and the caster to eventually become a part of the steel. This was to be accomplished by inserting an appropriately designed baffle into the tundish to chemically trap the inclusions and form accretion-like deposits on the baffle. The baffle was actually manufactured of a refractory similar to the alumina found in the accretions and turbulence was generated by incorporating multiple "zigzag" channels into the baffle. Computational fluid dynamic analysis was applied to the baffle/channel design to simulate the molten steel flow through the tundish and baffle channels. Actual field trials were completed at Timken Steel. Two separate field trials did not produce steel with any reduced inclusion content in the steel, even though the baffle design was modified after the first trial was unsuccessful. Suggestions for future research based on these principles are suggested.

OBJECTIVE OF THE RESEARCH

The project objective was to develop an effective chemical filtering system for significantly reducing the content of inclusion particles in the steel melts exiting the tundish for continuous casting. This project combined a multi-process approach that aimed to make significant progress toward an "inclusion-free" metal by incorporating several interdependent concepts to reduce the amounts and the sizes of inclusions in the molten steel exiting the tundish for the caster. The goal is to produce "cleaner" steel.

INTRODUCTION

One of the most critical aspects of steel quality is its cleanliness with regard to inclusion content. Inclusion particles in cast steel may originate from various sources within the molten steel before casting. Steel producers know that the presence of inclusions directly affects the quality of their products through the generation of defects, in the hot workability of the steel, and as the sources for fatigue crack initiation. Inclusions are also a serious problem in the formation of accretions in submerged entry nozzles (SENs) at tundish outlets. Clean steel, however, is usually defined by consumer demand rather than in terms of composition or inclusion levels because this definition depends on the final application of steel products. While total elimination of inclusion particles from steel is probably an unrealistic goal, the decrease, removal, and control of the inclusions in the cast steel is an important aspect in all steel production processes.

Physical sieving of the inclusion particles is impractical because the sieve will be rapidly clogged. Historically, various filtering techniques have been applied for the removal of inclusions from the molten steel in the tundish. These include foams or porous filters (Ichibashi, 1986) and processes utilizing various physical properties such as the bubble trapping of particles (Chevrier, 2000), floatation (He and Sahai, 1990), electro-magnetic separation (Taniguchi and Brimacombe, 1997), etc. However, these techniques produced limited success in attaining the required level of inclusion removal. The search for an alternative effective inclusion removal system from the molten steel in the tundish is a continuing and an active research area. The present investigation considers an alternative inclusion removal system from the molten steel while it is in the tundish.

A large portion of the inclusion particles in aluminum-killed molten steel poured into the tundish consists of the minerals spinel ($MgAl_2O_4$) and alumina (Al_2O_3) which are high melting point oxides that have a very strong affinity to adhere/bond to oxides (Itoh, Hino, and Ban-ya, 1997) as evident by the formation of accretions in the SEN. This bonding or chemical adherence is to be exploited in the proposed filtration/trapping technique for removing the inclusions from the steel. A refractory block of vertically stacked zigzag channels will be strategically placed across the steel flow direction within the tundish. The zigzag channel block may either be manufactured wholly of spinel or the channel surfaces may be coated with spinel. The concept is that the steel flow through the tortuous channels induces recirculation and increased turbulence so that the inclusion particles come in contact with the channel surfaces and adhere to them. Once the particles hit the channel surface, it is expected that they will chemically bond with the surface thereby being removed from the molten steel. This phenomenon actually occurs during the clogging of the SENs by the formation of accretions at the SEN exit. In principle, the

zigzag channel block may be physically removed from the tundish and replaced with a new block once the old block becomes clogged with trapped inclusions.

NUMERICAL MODELING

The success of physiochemical entrapment of inclusion particles from molten steel in the tundish must be evaluated in actual field trials with an industrial tundish. However, before the field trial, preliminary modeling studies of the actual design of the zigzag channels, the flow behavior of the steel with the channels, and the resulting trajectories of the inclusion particles are necessary to assess the potential effectiveness of the filtering system. This can be accomplished using numerical simulation/modeling of the tundish equipped with the zigzag channel inclusion trapping system. This section of the report describes such a numerical study about the feasibility of incorporating a proposed inclusion removal system in an actual industrial tundish. The flow behavior of the molten steel and the trajectories of the inclusion particles within the tundish and through the zigzag channels are numerically computed and the results are graphically presented.

Mathematical/numerical models for tundish flow analysis have been previously employed by several researchers. Chakraborty and Sahai (1991) in a study of the effects of turbulent collisions, re-oxidation, flotation, and inclusion size distribution, predicted the removal of alumina inclusions from molten steel in a continuous casting tundish. Shen, Khodadadi, Pien, and Lan (1994) completed turbulence measurements and also finite-element simulation for the tundish flow of aluminum and found favorable agreement between the experiment and prediction. Sheng and Jonsson (1999) conducted water modeling of the tundish flow and applied a three-dimensional transient mathematical model to observe significant buoyancy effects. Lopez-Ramirez, Morales, and Serrano (2000) performed numerical simulation of the effects of buoyancy forces and flow control devices on fluid flow and heat transfer in a tundish. Javurak, Kaufmann, Gerhard, and Philipp (2002) noticed that unsuitable flow patterns and turbulent particle diffusion were the reasons for unsatisfactory particle separation. They noted that the turbulent shear forces in the molten steel affects the coagulation of inclusions in the tundish. Nakashima, Tanaka, Fukuda, Kiyose, and Yamada (2003) observed that in an actual tundish the turbulence dissipation rate is largest near the inlet nozzle, but extremely small in all other regions. They studied various design parameters such as the inlet shroud immersion depth, different outlet positions, and different designs of the pour boxes for flow optimization with various turbulence models. Jha and Dash (2002, 2004) evaluated different turbulence models of the $k-\varepsilon$ family for the prediction of tundish flow and concluded that the RNG $k-\varepsilon$ model performs better than the other variants of the $k-\varepsilon$ model. Amberg and Shiomi (2005) studied the effect of convection on generic solidification problems. Ludwig, Gruber-Pretzler, Wu, Kuhn, and Riedle (2005) numerically investigated the formation of macrosegregations during continuous casting of Sn-Bronze and discussed the impact of different convection types like inlet flow, thermal and solutal buoyancy flow, and feeding flow using the FLUENT CFD code. Abhilash, Joseph, and Krishna (2006) used artificial neural networks algorithm for the prediction of dendritic parameters and macro hardness variation in permanent mould castings. Hong, Zhu, and Lee (2006) performed the modeling of dendritic growth in alloy solidification with melt convection.

The present study consists of two parts. The first is the hydrodynamic design optimization of the zigzag channel. It is performed numerically considering the two-dimensional geometry of a single zigzag channel. Suitable channel design is decided on the basis of results of a parametric study and examination of the flow behavior and particle trajectories within the channel. In the second part, a numerical model for a three-dimensional industrial tundish is developed. Steel flow and particle trajectories in the tundish are computed and analyzed. Finally, the tundish flow model is modified by inserting a vertically stacked block containing multiple zigzag channels with the same geometrical design obtained in part one of the study. The flow and particle trajectory computations are then repeated. The results are analyzed and the feasibility of the proposed inclusion trapping/removal technique is discussed.

The tundish used in the model is a delta tundish that is symmetrical about the mid-plane through the inlet shroud. Because of this symmetry only half of the tundish is modeled. The geometry of the symmetric half of the tundish and its modified version with the block of zigzag channel insert in place is shown in Fig. 1.

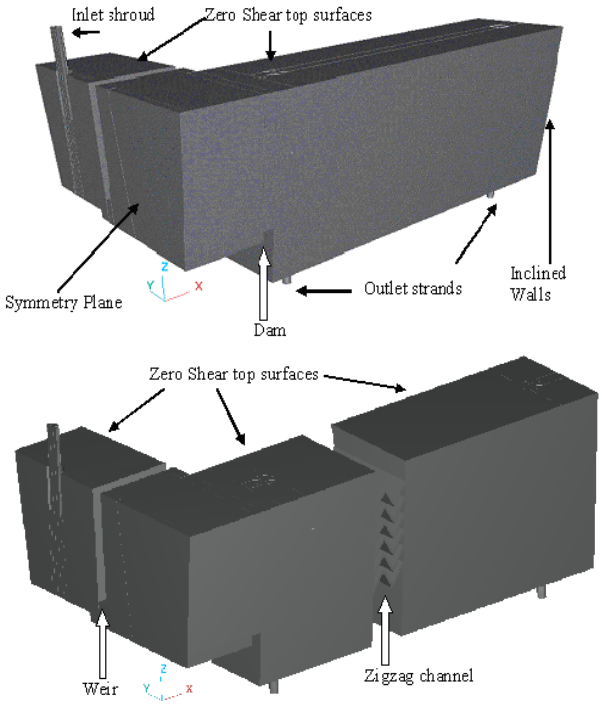

Figure 1: The modeled tundish schematic showing the geometric features; the bottom figure shows the tundish with the zigzag channel block insert in place.

The main tundish tank is in the longitudinal direction while the pouring block containing the inlet shroud is projected in the span wise direction. It is separated from the main tundish by a weir. The entering steel flow is poured through the inlet shroud onto the pouring block. The steel flow passes beneath the weir and is divided into to equal parts and turns longitudinally and flows over a span-wide small dam into the main tundish tank, then exits through the two outlet strands at the bottom on each side. One of the

outlets is located near the dam while the other outlet is further downstream close to the end wall. The zigzag channel inclusion trap is inserted at a strategic position in between the two outlets in the modified tundish model.

In order to impose a Cartesian coordinate system onto the tundish geometry, the *x* direction is assigned parallel to the longitudinal direction of the main tundish cavity. The *y* direction is assigned span-wise and *z* direction is the vertical. The origin of the coordinate system is positioned at the intersection of the lower edge of the symmetry plane and the vertical mid-plane through the main tundish cavity, hence $y = 0$ on that plane.

Mathematical Formulation

Governing equations for fluid motion. The governing equations for the incompressible flow consist of the conservation of mass and the Reynolds averaged Navier-Stokes (RANS) equations. They are written in the indicial notation as the following:

$$\frac{\partial \bar{u}_i}{\partial x_i} = 0 \tag{1}$$

$$\frac{\partial(\rho \bar{u}_i)}{\partial t} + \frac{\partial\left(\rho \bar{u}_i \bar{u}_j\right)}{\partial x_j} = \rho \bar{f}_i + \frac{\partial}{\partial x_j}\left[-\bar{p}\delta_{ij} + \mu\left(\frac{\partial \bar{u}_i}{\partial x_j} + \frac{\partial \bar{u}_j}{\partial x_i}\right) - \rho\overline{u_i' u'}_j \right] \tag{2}$$

where $\bar{u}_i$ are the mean velocity components, x_i are the coordinate directions, ρ is the fluid density, t is the time, $\bar{f}_i$ is the body force per unit mass, $\bar{p}$ is the mean pressure, δ_{ij} is the Kronecker delta, μ is the fluid dynamic viscosity, and u_i' are the fluctuating velocity components. The Reynolds stresses in the right hand side of Eq. (2) are:

$$-\rho\overline{u_i' u_j'} = \mu_t\left(\frac{\partial \bar{u}_i}{\partial x_j} + \frac{\partial \bar{u}_j}{\partial x_i}\right) - \frac{2}{3}\rho k \delta_{ij} \tag{3}$$

where μ_t is the turbulent eddy viscosity and k is the kinetic energy of turbulence. Applying the standard $k-\varepsilon$ model (Launder and Spalding, 1994), the eddy viscosity is given as

$$\mu_t = \rho C_\mu \frac{k^2}{\varepsilon} \tag{4}$$

where ε is the turbulence dissipation. The kinetic energy of turbulence, k, and its dissipation rate, ε, are obtained by solving their respective transport equations whose modeled forms are given as

$$\frac{\partial(\rho k)}{\partial t} + \frac{\partial\left(\rho k \bar{u}_j\right)}{\partial x_j} = \frac{\partial}{\partial x_j}\left[\left(\mu + \frac{\mu_t}{\sigma_k}\right)\frac{\partial k}{\partial x_j}\right] + P_k - \rho\varepsilon \tag{5}$$

and

$$\frac{\partial(\rho \varepsilon)}{\partial t} + \frac{\partial\left(\rho \varepsilon \bar{u}_j\right)}{\partial x_j} = \frac{\partial}{\partial x_j}\left[\left(\mu + \frac{\mu_t}{\sigma_\varepsilon}\right)\frac{\partial \varepsilon}{\partial x_j}\right] + C_{1\varepsilon} P_k \frac{\varepsilon}{k} - C_{2\varepsilon}\rho\frac{\varepsilon^2}{k} \tag{6}$$

where the production term $P_k = -\rho\overline{u_i'u_j'}\left(\partial\bar{u}_j/\partial\bar{u}_i\right)$. The model constants in Eqs. (5) and (6) are; $C_\mu = 0.09$, $C_{1\varepsilon} = 1.44$, $C_{2\varepsilon} = 1.92$, $\sigma_k = 1$, and $\sigma_\varepsilon = 1.3$. Standard wall function prescriptions (Launder and Spalding, 1974) at the wall are used to solve the equations.

Governing equation for particle motion in fluid. Particle motion in a fluid is governed by the Lagrangian equation of motion

$$m_p \frac{\partial U_{pi}}{\partial t} = F_{Wi} + F_{Di} + F_{Pi} + F_{SLi} + F_{MLi} \tag{7}$$

where m_p is the mass of the particle, U_p is the particle velocity vector, F_W is the body force term expressing the difference between the weight and the buoyancy force on the particle, F_D is the drag force, F_P is the pressure gradient force, F_{SL} is the Saffman lift force, and F_{ML} is the Magnus lift force. The subscript index *i* is the tensor index and stands for the *i*th coordinate direction.

The body force is given by

$$F_{Wi} = \frac{\pi}{6} d_p^3 (\rho_p - \rho_f) g_i \tag{8}$$

where g_i is the component of gravitational acceleration in the *i*th direction.

The drag force is given by

$$F_{Di} = \frac{1}{2} \rho_f U_{ri} \,|U_{ri}|\, A_{pi} C_D \tag{9}$$

where ρ_f is fluid density, U_r is the relative fluid velocity with respect to the particle, A_{pi} is the frontal area of the particle as seen from the *i*th direction, and C_D is the drag coefficient. The relative fluid velocity vector is given by $U_r = U_f - U_p$ where U_f is the fluid velocity vector. The *i*th component of U_r is used in Eq. (9). The particle shape is considered spherical for which the drag coefficient, C_D, is given by $24/\mathrm{Re}_{pi}$. This assumes that the particle Reynolds number, Re_{pi}, is very small. The particle Reynolds number is defined in terms of the relative velocity (U_{ri}) and particle diameter (d_p) as $\rho_f U_{ri} d_p / \mu$. Other prescriptions for C_D over a wide range of Reynolds number are available in Clift, Grace, and Weber (1978).

The pressure gradient force on the particle is given by

$$F_{Pi} = -(\pi/6) d_p^3 \left(\partial p / \partial x_i\right) \tag{10}$$

Small particles in a shear field experience a lift force perpendicular to the flow direction of the fluid phase. This lift originates from the inertia effects in the viscous flow around the particle. The expression for the inertial shear lift was first presented by Saffman (1965). It is written in the following form (Ran, Zhang, Tang, and Xin, 2006),

$$F_{SLi} = 1.615(\rho\mu)^{0.5} d_p^2 U_{rj} \left|\frac{\partial U_{rj}}{dx_i}\right|^{0.5} \mathrm{sgn}\left(\frac{\partial U_{rj}}{dx_i}\right) \tag{11}$$

where the "sgn" term in the right hand side is either 1 or -1 depending on whether the derivative term in its argument is positive or negative.

Local flow vorticity may cause the particles to spin. For spinning particles in a fluid stream, an additional force perpendicular to the streamwise direction is created. This is called the Magnus lift force. The Magnus lift force on the particles spinning at an angular velocity vector, ω_p, initiated by the fluid rotation is expressed as (Lun and Liu, 1997)

$$F_{ML} = \frac{1}{2}\rho_f (U_r \cdot U_r)\frac{\pi d_p^2}{4} C_{ML} \frac{\omega_p \times U_r}{|\omega_p||U_r|} \tag{12}$$

The angular velocity vector of the particle can be obtained from the local vorticity as $\omega_p = (1/2)\nabla \times U_f$ and the coefficient C_{ML} is given by

$$C_{LM} = d_p|\omega_p|/|U_r| \tag{13a}$$

if $\mathrm{Re}_p \le 1$, and

$$C_{LM} = d_p|\omega_p|/|U_r|\left(0.178 + 0.822\mathrm{Re}_p^{-0.522}\right) \tag{13b}$$

if $1 < \mathrm{Re}_p < 1000$.

It is to be noted that the *i*th component of F_{ML} must be used in Eq. (7) and Re_p is defined as $\rho_f U_r d_p / \mu$.

The particle trajectories are also affected by turbulent eddies which can be incorporated by numerically generating the fluctuating velocity components u_i', and adding those to the local mean fluid velocity components, U_{fi}, for every time step integration of Eq. (7) [Schwarze, Obermeier, and Janke (2001) and Varga-Zamora, Morales, Diaz-Cruz, Palafox-Ramos and Demedices (2003)]. Therefore, the inclusion particles will be more dispersed and the chances of the particles impacting the channel surfaces will be increased. This effect will also aid the inclusion particles in getting out of the "closed streamlines" encompassing the recirculation regions. The fluctuating velocity components can be generated as $u_i' = \xi\sqrt{k}$ where ξ is the product of a random number between -1 and 1 and an empirical constant. That turbulent dispersion effect, however, has not been considered in the present study.

Details of the numerical process. The governing equations were solved through the application of the commercial computational fluid dynamics code, CFD-ACE+^{TM} (ESI-CFD, 2006). The flow domain was divided into small finite volume cells with an unstructured tetrahedral mesh. The governing RANS equations and the transport equations for k and ε were integrated over each cell to generate a linear system of algebraic equations. These were then solved sequentially. The convective fluxes in the transport equations were calculated using the second-order upwind scheme while the diffusive fluxes are calculated using the central differencing scheme. The linear system for each transport equation was solved iteratively until convergence when the residuals are very small for each equation. The pressure velocity coupling was achieved using the well known SIMPLE method (Patankar, 1979). A time marching procedure with first-order accurate forward differencing time integration was applied to reach the steady-state solution until the variation of each variable between two successive time-steps is insignificant over all cells.

For the simulations, the density and viscosity of molten steel was specified to be 7000 kg/m^3 and 0.0055 Pa s, respectively. An assumed temperature of 1875 K was used.

The particle trajectories were calculated by activating the relevant component of the CFD-ACE+^{TM} code. Once the steady-state hydrodynamic field was solved, it was then frozen and the particles were introduced into this hydrodynamic field with the local initial velocity for the specific point of introduction. Time integration of Eq. (7) governing the particle motion was then used to calculate particle locations for each particle using small time steps. The locations were then joined by a curve to display the particle trajectories. No chemistry/chemical kinetics model for the particle-particle coagulation/agglomeration or particle to wall adsorption was used to compute the particle trajectories. For the particle trajectory calculation, one way coupling was assumed, meaning the particle motion is affected by the hydrodynamic field, but the hydrodynamic field is not affected by the particle motion. This is a valid assumption since the particle distribution in the molten steel is a very dilute one of well dispersed particles. Also particle to particle collision was not considered in the calculations. However, particle to wall collision was considered through the use of a coefficient of restitution, which has a value between 0 and 1. When the coefficient of restitution is zero, it is a fully plastic collision in which case the particle is assumed to stick to the wall after collision. On the other hand if it is 1, it is a fully elastic condition in which case the particle bounces back with the same speed as before the collision. The fully plastic condition for the particle to channel wall collision by setting the coefficient of restitution to 1 will be used later to simulate the bonding of the particles with the channel walls in lieu of any model to describe the inclusion capture rate. In all trajectory calculation, spherical particles of 1-100 μm diameter with a mass density of 4000 kg/m^3 were considered. This density is representative of typical oxide inclusion particles.

RESULTS OF NUMERICAL MODELING AND DISCUSSION

Zigzag Channel Design

As mentioned earlier, the zigzag channel insert in the tundish is the core of the inclusion filtering/trapping technique. The objective was to utilize the increased recirculation and turbulence of the molten steel while passing through the zigzag channel to bring the inclusion particles in contact with the channel surfaces. The inclusions are then expected to chemically react with the channel surface and bond to it and thus be trapped. It is essentially duplicating the conditions which create the accretions at the SEN exit. As such, a detailed simulation of the flow behavior and particle trajectories through the zigzag channel is required in order to optimize the design of the channel configuration which will be used in an actual tundish. First, a two-dimensional channel design, as shown in Fig. 2, is adopted to evaluate its effectiveness even though the actual tundish flow is three-dimensional. This, however, is not a gross simplification since the flow through the three-dimensional zigzag channel will be basically a two-dimensional one, i.e., the variation in the span-wise direction within the channels will be insignificant. This particular configuration for the zigzag channel was chosen to facilitate the ease of fabrication of the channel insert and to minimize the space for the placement of the insert in the existing tundish.

The channel is to be placed within the tundish where the general flow direction is upward and closely matches the entry channel angle. This is to be determined by examining the three-dimensional simulation of the tundish flow without the presence of the zigzag channel. The zigzag channel exit is directed upward so that the exit flow reaches the slag layer and any of the remaining inclusion particles that escape being trapped by the channel have an opportunity to react with the slag and be removed there as in the case for the standard float-out method of inclusion removal.

Two important geometric parameters for the channel design/optimization study are the channel spacing, h, and the zigzag angle, θ, as shown in Fig.2. The study was performed through numerical simulation of the steel flow through the channel with the calculation of the particle trajectories for various combinations of these basic geometric parameters. Results were compared and analyzed and an optimum pair of these parameters was determined for the channel design which was used later in the three-dimensional simulation of the actual industrial tundish.

In the flow simulation, no-slip boundary conditions were used at the channel walls and constant pressure conditions were specified at the outlet. The inlet velocity components were derived/extracted from the three-dimensional tundish (without the zigzag channels) flow simulation at the location where the channel insert was to be placed. A systematic grid refinement study was conducted to obtain the optimum mesh distribution. The nodes are clustered towards the channel walls. Four different channel spacings, 0.0127, 0.0254,

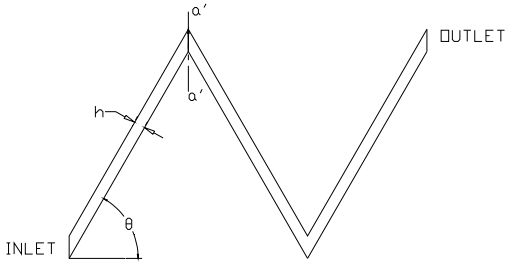

Figure 2: Schematic diagram of the two-dimensional zigzag channel.

0.0381, and 0.0508 m (0.5, 1, 1.5, and 2 in.), and four different zigzag angles (30º, 45º, 60º and 70º) were considered resulting in a total of 16 different simulations.

The flow streamlines for each of the 16 channel configurations are shown in Fig. 3 where it is observed that the flow recirculation occurs at the vertices of the zigzag channel and on the opposite walls immediately downstream of the vertices. The extent of the recirculation regions in the domain increases with increasing passage width for each particular zigzag angle. Excessive recirculation within the channel will be detrimental to the objective of bringing the particles into contact with the channel surfaces. A representative estimate of the percent recirculation volumes compared to the total volume within the channel with a 0.0254 m (1 in) spacing for various zigzag angles is presented in Table 1. The estimate was completed by plotting the streamlines on a fine graph paper and counting the number of small squares encircled by the recirculation bubbles. From these results it is noticed that while the recirculation volume is a maximum for the 45° angle, it is similar to that for the 60° and 70° zigzag angles.

For the optimum channel design, the pressure drop across the channel must not be excessive. The pressure drop, as a function of the zigzag angle, θ, is presented for various passage spacings in Fig. 4. While the pressure drop is not strongly affected by the passage spacing; it increases significantly with the zigzag angle. The pressure drop beyond a 60° zigzag angle seems to be excessive.

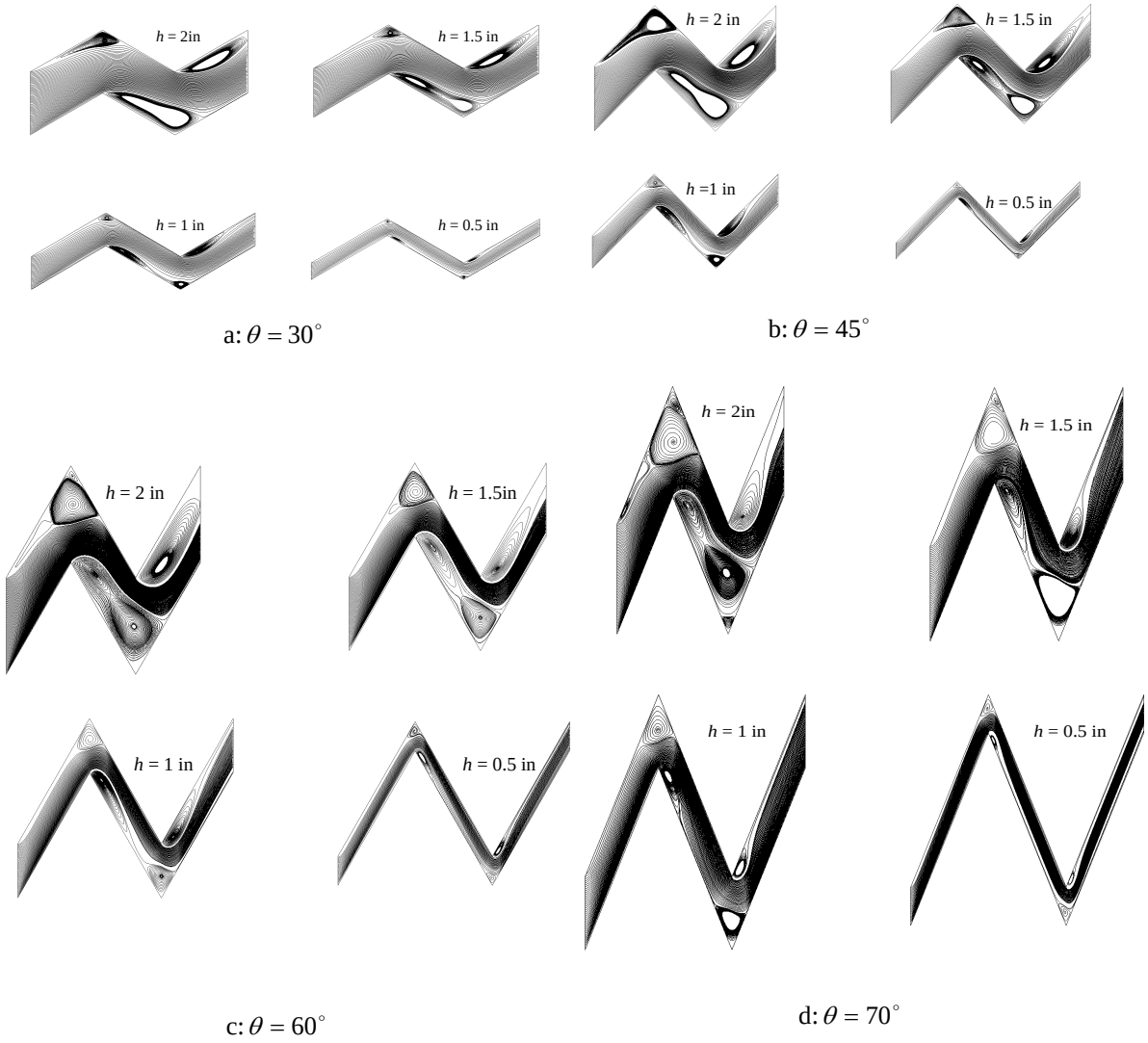

Figure 3: Streamlines in the zigzag channel.

The most important feature to consider for the design of the zigzag channel to fulfill the objective of this research is the particle trajectory history through the channel. To this effect the trajectories of particles inside the channel were determined by applying the particle dynamics equation [Eq. (4)]. The particle trajectories for a channel with a 0.0254 m (1 in) spacing and 60° angle are shown in Fig. 5. To understand the effects of the particle size on the trajectories, the diameter of the particles were varied as 25, 50, 75, and 100 μm. Particle trajectories depend upon the flow field in the zigzag channel and the various forces including the buoyancy force exerted on the particle. In general, larger particles tend to rise to the top surface of the channel near the inlet section which is desirable for the objective. This can be directly attributed to the larger buoyancy force

exerted on the larger size particles. Smaller particles, experiencing lesser buoyancy force, tend to flow along with the fluid and then exit through the channel outlet. However, many smaller particles impact the channel wall especially on the second inclined top surface and the third inclined bottom surface during their travel through the zigzag channel.

Table 1: Recirculation volume estimates in percent of total channel volume for a channel with 1 inch spacing.

Zigzag angle	Percent recirculation volume
30º	7.65
45º	20.14
60º	16.23
70º	16.31

Considering the effects of various geometric parameters such as the zigzag angle and passage spacing and fluid dynamic factors such as the recirculation volume, particle behavior, and pressure drop across the channel, a channel having a zigzag angle of 60° with a passage spacing of about 0.0254 m (1 in) is a near optimum channel design for effective chemical trapping of the inclusions. As such, this configuration of the zigzag channel was recommended for implementation in the complete three-dimensional model of the tundish flow simulation.

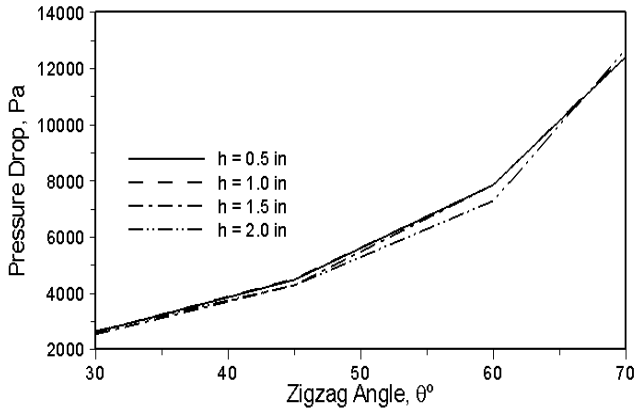

Figure 4: Pressure drop across the channel.

Three-Dimensional Tundish

Two different numerical models; one of the existing tundish and the other of the tundish with the zigzag channel block in place, were considered. The hydrodynamic field in the existing tundish was first calculated and analyzed to understand the overall tundish flow

behavior and to identify a strategic location for the placement of the zigzag channel block within the tundish.

The unstructured tetrahedral meshes for both models, as shown in Fig. 6, were generated by the mesh generation module of the CFD-ACE+^{TM} code. A dense mesh was employed near to the inlet shroud, within the pour pad, near to the outlet nozzles, and near all of the walls of the tundish. The intense computational demand of these did not allow a systematic grid refinement study to be performed. However, after few preliminary trials, a mesh with ~150,000 cells was deemed satisfactory for the feasibility study as the quantitative accuracy was not a major concern at this point.

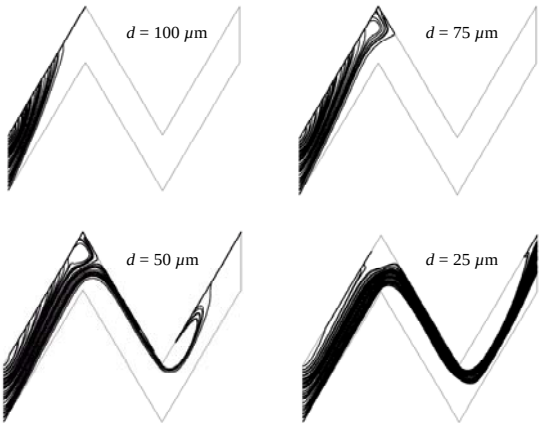

Figure 5: Particle trajectories in the zigzag channel with 1 inch spacing and 60° angle.

A uniform volumetric flow rate of 0.00355 m^3/s obtained from real tundish data was specified at the inlet. This translated to a uniform inlet velocity of 0.628 m/s downward with an inlet Reynolds number of ~40,000. Constant pressure (0.0 Pa) conditions were specified at the outlet. No-slip conditions were imposed at all of the walls except for the top surface and the symmetry plane where zero shear stress and zero normal velocity conditions were imposed (Ilegbusi and Szekely, 1987). Isothermal conditions were assumed and as such it was not necessary to solve the energy equation.

Tundish flow without the zigzag channel insert. Within the pour pad chamber of the tundish, which is contained by the weir, the fluid jet from the inlet shroud impinges on the bottom, spreads outward radially, bounces back ascending near to the chamber walls, hits the top surface, goes down again, and ultimately exits the pour pad chamber through the opening beneath the weir. This produces a vigorous turbulent intermixing of the fluid and inclusion particles within the inlet chamber. This is depicted by the streamtrace plots within the pour pad chamber using mass less particles of negligible diameter released at the inlet. This pattern is shown in Fig. 7.

The overall flow pattern throughout the tundish can be visualized in the sample streamtrace plots presented in Fig. 8. A strong helical form of motion of the fluid before its entry into the main tundish chamber is noticeable. In the main tundish cavity, however, the flow does not appear quite as erratic as it is in the inlet zone. This is because of the large reduction of the flow velocity magnitude.

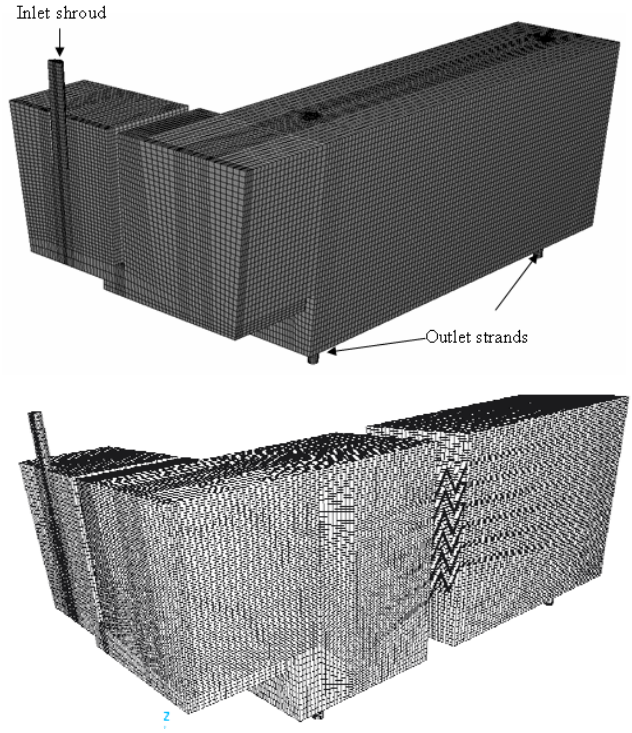

Figure 6: Mesh for tundish models; top – without the zigzag channel, bottom – with the zigzag channel block.

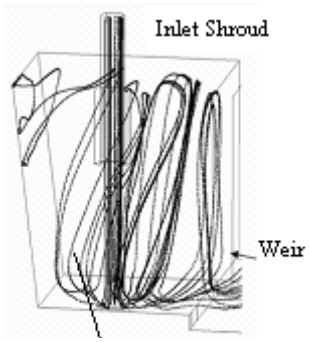

Figure 7: Streamtrace plots within the pour pad.

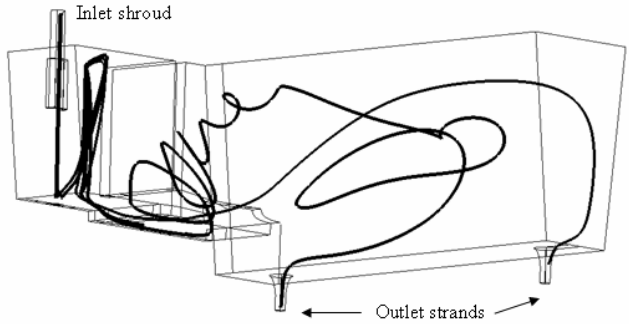

Figure 8: Streamtraces depicting the flow from the inlet shroud to the outlet nozzles.

As expected, the geometry of the tundish furniture has a profound influence on the flow behavior of the molten steel within the tundish. The purpose of the small span-wise dam at the entry to the main tundish cavity is to prevent the molten steel from going directly to the outlet nozzles and short-circuiting the overall flow pattern. This is clearly depicted by the streamtrace plots shown in Fig. 9. The dam also guides the flow upwards which has two purposes. First, it increases the residence time and second, the steel flow comes into contact with the slag layer where the inclusion particles are able to react and coagulate with the slag, thereby reducing the inclusion particle content to some extent.

The turbulence level in the fluid stream is a quantity of interest here. A contour plot of the kinetic energy of turbulence on a vertical *xz* plane through the tundish cavity is presented in Fig. 10. It shows large gradients and peaks at the entry region to the main tundish cavity and again in the vicinity of the outlet area.

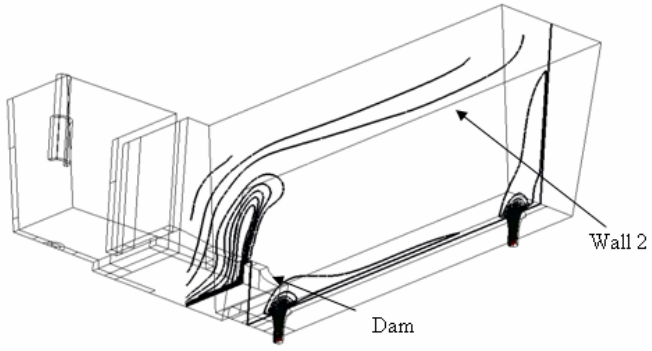

Figure 9: Streamtraces depicting the flow over the small dam.

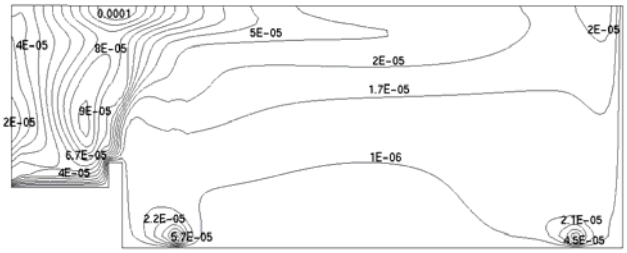

Figure 10: Contours of the turbulent kinetic energy (m^2/s^2) on a *xz* plane through the tundish cavity.

Tundish with a zigzag channel insert. Because of the presence of the zigzag channel block, the main tundish cavity is conveniently divided into two chambers between which the channel block acts as a flow barrier. Pre-simulation suspicions were that this might severely reduce the flow through the downstream outlet nozzle near the end wall. This, however, does not happen as the flow through the downstream outlet is reduced only by about 5%. A streamtrace plot through the tundish is shown in Fig. 11. This shows the flow pattern differences in the tundish compared to that in Fig. 8 which is for the same tundish without the zigzag channel. Erratic motion in the entry region and a large recirculation zone occurs in the second portion of the main tundish cavity downstream of the zigzag channel block.

A sample plot of the turbulent kinetic energy for the same *xz* plane as in Fig 10 is shown in Fig. 12. Very large gradients of the turbulent kinetic energy upstream bottom part of the dam, top of the dam, near the outlets, and on the upstream side of the zigzag channel block is noticeable. The turbulence intensity distribution is significantly different from that in Fig 10 for the case of the tundish without the zigzag channel block.

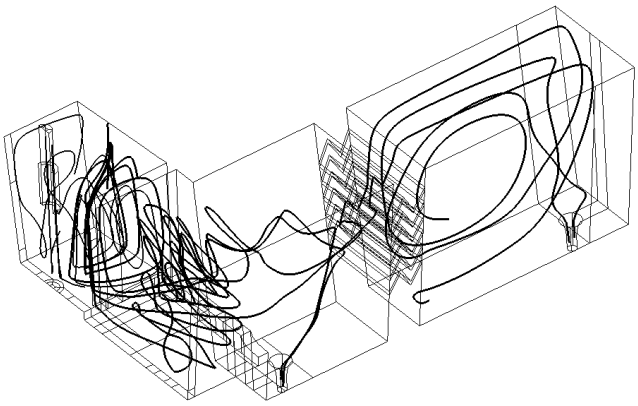

Figure 11: Streamtraces in the tundish with the zigzag channel.

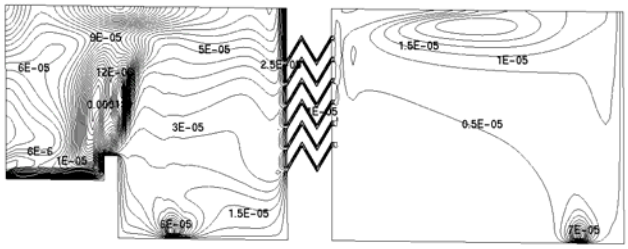

Figure 12: Contours of the turbulent kinetic energy (m^2/s^2) on a *xz* plane through the tundish cavity.

Particle trajectories in the tundish with the zigzag channel. Computation and visualization of the particle trajectories in the tundish equipped with the zigzag channel block is the most important aspect of this study since that will determine the ultimate feasibility of the inclusion trapping and filtering technique. For that reason extensive computation of the particle trajectories and their critical visualization were performed. Initially, the coefficient of restitution for the particle to zigzag channel wall collision was set to 1 for which case the particles bounce back from the wall with the same speed as before the wall collision, as mentioned in section 2.3. Particles having uniform diameters were released at the inlet and the trajectories were computed as they passed through the flow domain. The trajectories for 100 μm and 75 μm diameter particles are depicted in Figs. 13 and 14. Very erratic and irregular motion of the particles in the entry region and in the main tundish cavity upstream of the zigzag channel is evident. This is because of the erratic motion of the fluid phase (the molten steel) in those regions. In the portion of the cavity downstream from the zigzag channel, the larger particles (100 μm) have relatively smooth trajectories (Fig. 13) compared with the smaller (75 μm) particles (Fig. 14).

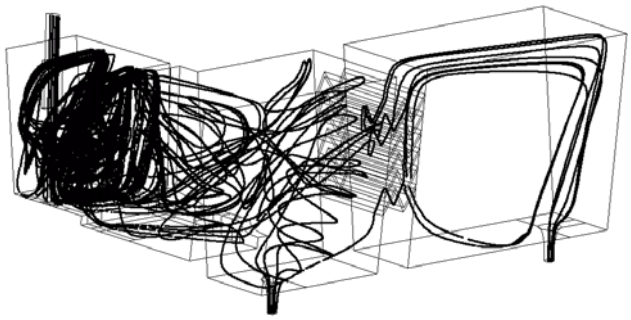

Figure 13: Trajectories of 100 μm diameter particles when the coefficient restitution for wall collision is set to 1.

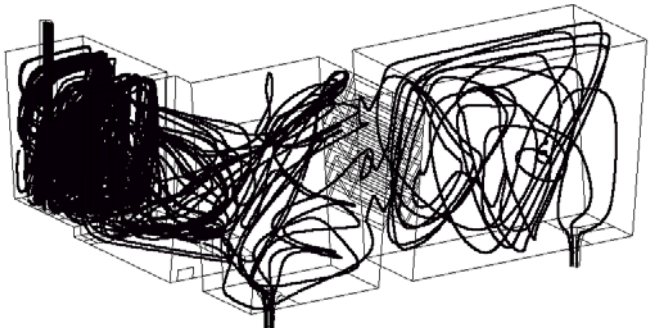

Figure 14: Trajectories of 75 μm diameter particles when the coefficient restitution for wall collision is set to 1.

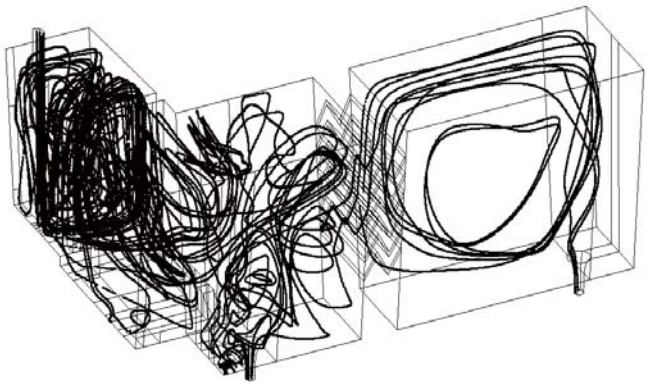

Figure 15: Trajectories of 1-100 μm diameter particles when the coefficient restitution for wall collision is set to 1.

Trajectories for a distribution of particles of various diameters (1-100 μm) released at the inlet are shown in Fig. 15. It has the same general trend as Figs. 13 and 14. The same situations are repeated with the coefficient of restitution for the particles to the zigzag channel wall collision set equal to zero. This mimics total particle adsorption at the wall in an *ad-hoc* manner. The particle trajectories for this case are shown in Fig. 16. It can be seen that none of the particles pass through the zigzag channel block into the downstream

portion of the cavity. This is quite remarkable in the sense that it demonstrates, albeit in a simulated fashion, the effectiveness of the zigzag channel surface in trapping the inclusion particles. It is thus expected that the proposed filtering technique has the potential to be successful. It will depend on the capture efficiency of the zigzag channel trap.

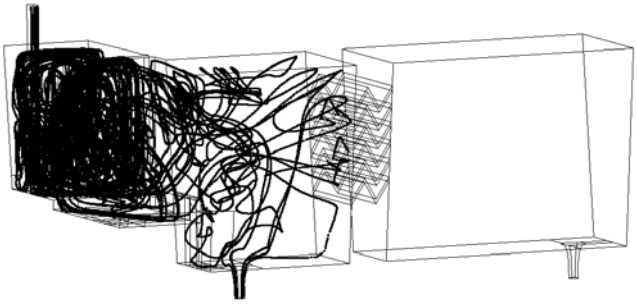

Figure 16: Trajectories of 1-100 μm diameter particles when the coefficient restitution for wall collision is set to 0.

Summary of the Numerical Study

A physical-chemical filtering system for the removal of inclusion particles from molten steel in the tundish was investigated. The molten steel will be directed through zigzag channels in the tundish furniture. The inclusion particles are expected to come in contact with the zigzag channel surfaces while passing through them because of the increased recirculation and turbulence. The inclusion particles are expected to stick to the zigzag channel surfaces and bond and get trapped there. The feasibility of the filtering system has been evaluated numerically and the results are reported in this study. The flow field in the tundish was computed by solving the incompressible RANS equations employing the standard $k-\varepsilon$ turbulence model. The particle trajectories were computed by solving a Lagrangian particle dynamics equation where the particles are subjected to various physical and hydrodynamic forces. The trajectories are then visualized and critically examined to assess the effectiveness of the filtering system.

Design optimization of the zigzag channel was performed by first computing the flow through a two dimensional zigzag channel and then computing the particle trajectories through the channels. A channel with 60º zigzag angle and 0.0254 m (1 in) channel spacing was deemed satisfactory for the purpose. A channel block consisting of the same channel design was then inserted into a three-dimensional model of an existing continuous casting tundish. The hydrodynamic field and the particle trajectories in the modified tundish model were then calculated and examined. It is concluded that the proposed filtering technique will be effective in removing the inclusion particles in the tundish. The actual physical verification of the effectiveness of the filtering system is pursued in the next phase of the project in field tests in the Timken plant.

FIELD TEST IN TIMKEN STEEL COMPANY

On the basis of the computer modeling of the tundish flow for the tundish, specifications for the zigzag channel baffle were provided to ANH Refractories (formerly North American Refractories) for their manufacture of the zigzag baffle to fit in the Timken tundish. During the testing, ANH produced two baffles; the second had smaller channel (0.5 inch spacing) to obtain greater turbulence within the channels, presumably to promote inclusion removal. The second baffle was produced when there was no evidence of inclusion trapping from the initial baffle with the larger channel (1 inch spacing). Figures 17 illustrate the schematic drawings of the baffle design, while Figure 18 shows the actual baffle. Neither of the two baffles in their separate tests showed any evidence of accretion formation within the channels from the deposition of inclusions from the steel as it flowed through the tundish.

As Timken had a multi-strand tundish, it was relatively easy to baffle one of the strands and compare its inclusion contents with that of an unbaffled strand. Figure 19 shows the SEM inclusion counts for the steel from the tundish, high counts yellow squares, with those from strand #1 which contained the second reduced channel size baffle and strand #4, which did not have the baffle in the flow stream of the molten steel. There was essentially no reduction of the oxide inclusion content from the baffle in the molten steel stream through the tundish. Table 2 and the total oxygen contents shown in Figure 20 also suggest that there was no removal of inclusions from the molten steel during the tests.

It must be concluded that there is no evidence that the presence of the baffle reduced the inclusion content of the steel produced from strand #1 relative to that of strand #4, simultaneously from the same tundish. The presence of the baffle did not reduce the inclusion content of the steel.

Although there was no reduction of the inclusion content, these tests do not disprove the basic concept of transferring the turbulence from the bottom of the SEN to within the tundish to remove inclusions from the molten steel. These trial runs did not produce any accretions in the baffles, nor did they produce any accretions with the SEN's in any of the multiple strands. This is not necessarily surprising, for accretion formation from deposit of the inclusions within the steel does not occur for every melt, just a few. It is entirely possible that neither of the two heats were prone to the inclusion formation of accretions. It is entirely possible that the lack of inclusion trapping and the lack of any accretion formation either, was the result of the particular heats of molten steel.

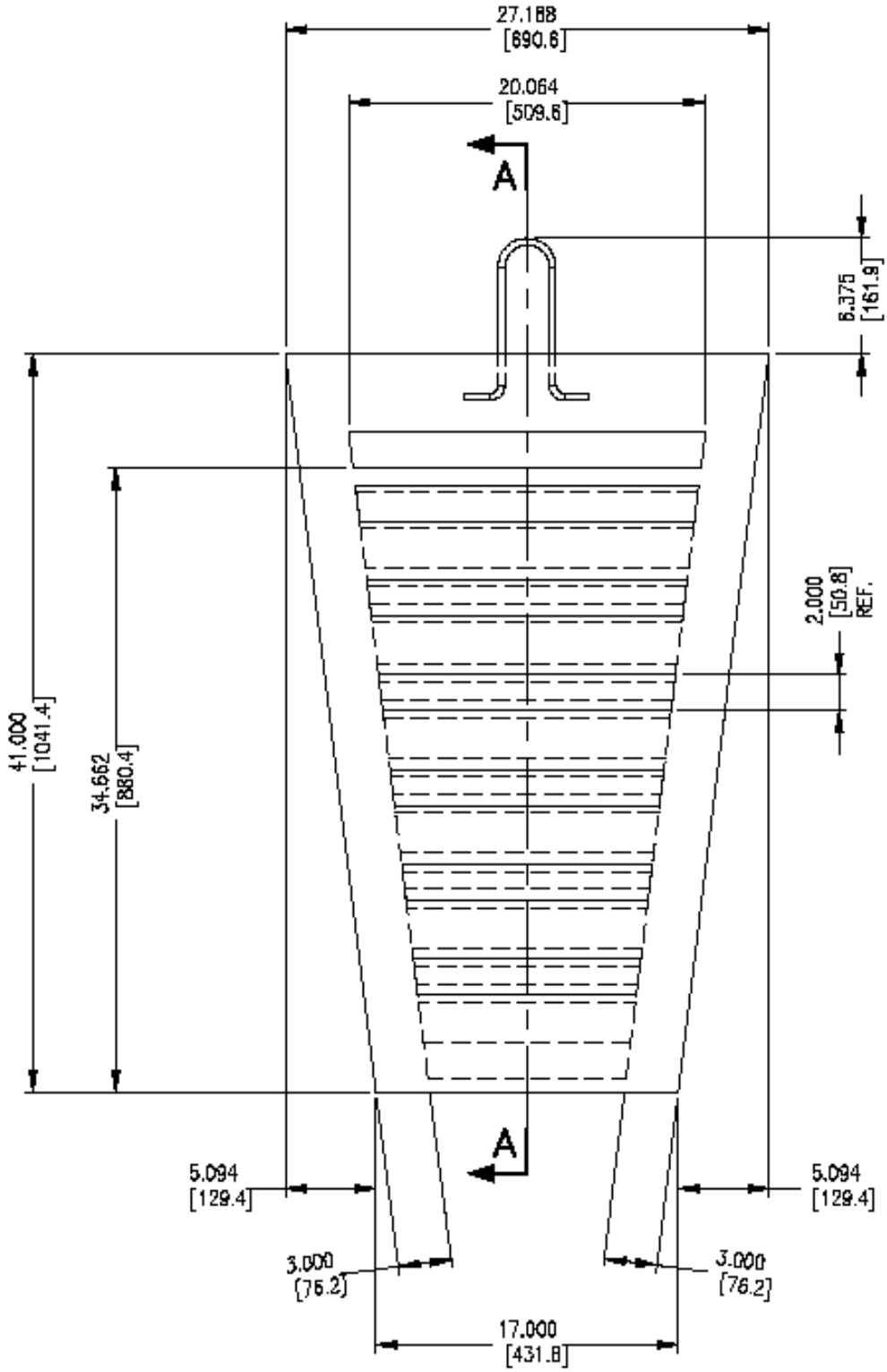

Figure 17(a): Detail drawing of the zigzag channel.

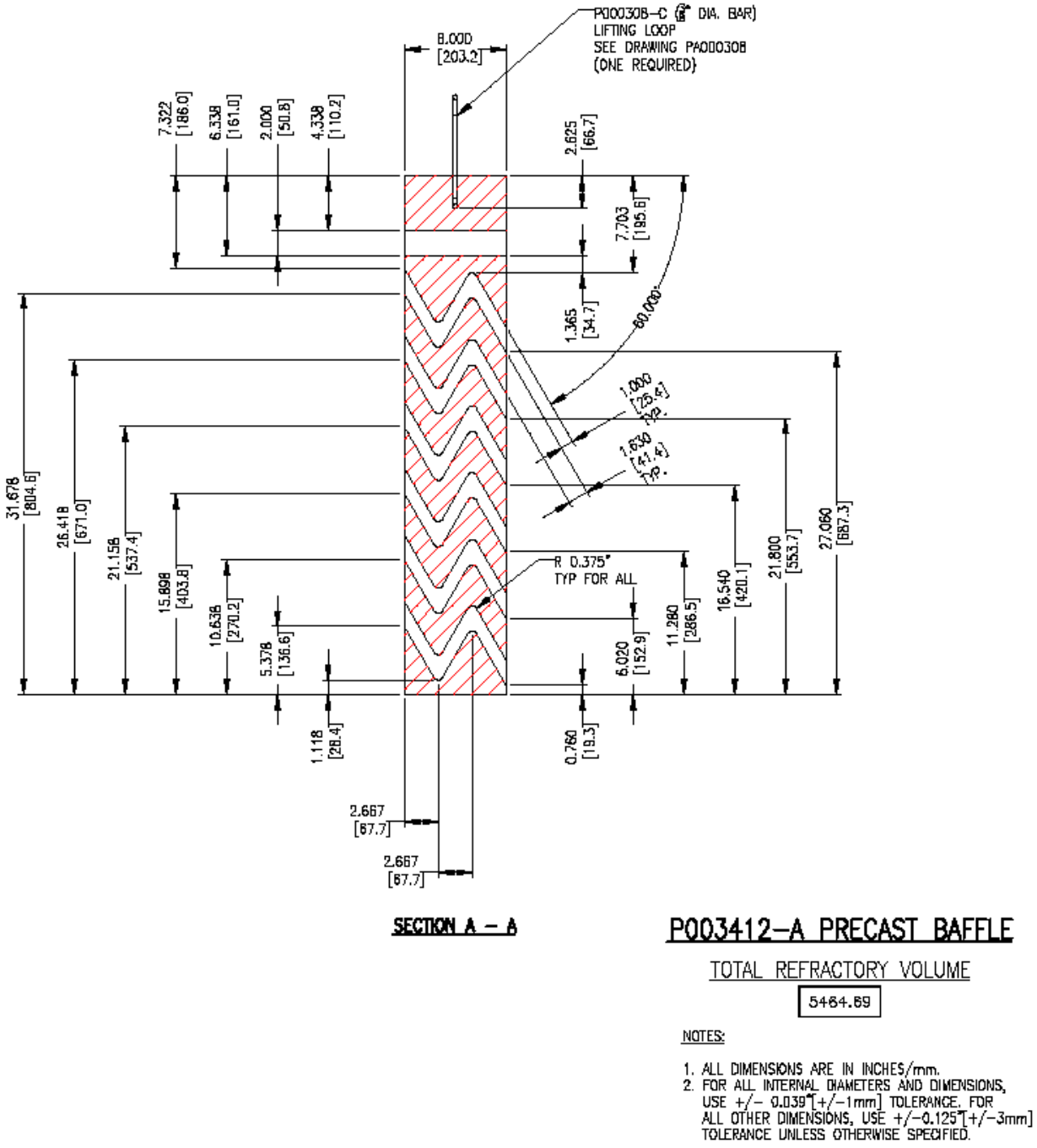

Figure 17(b): Sectional view of the zigzag channel.

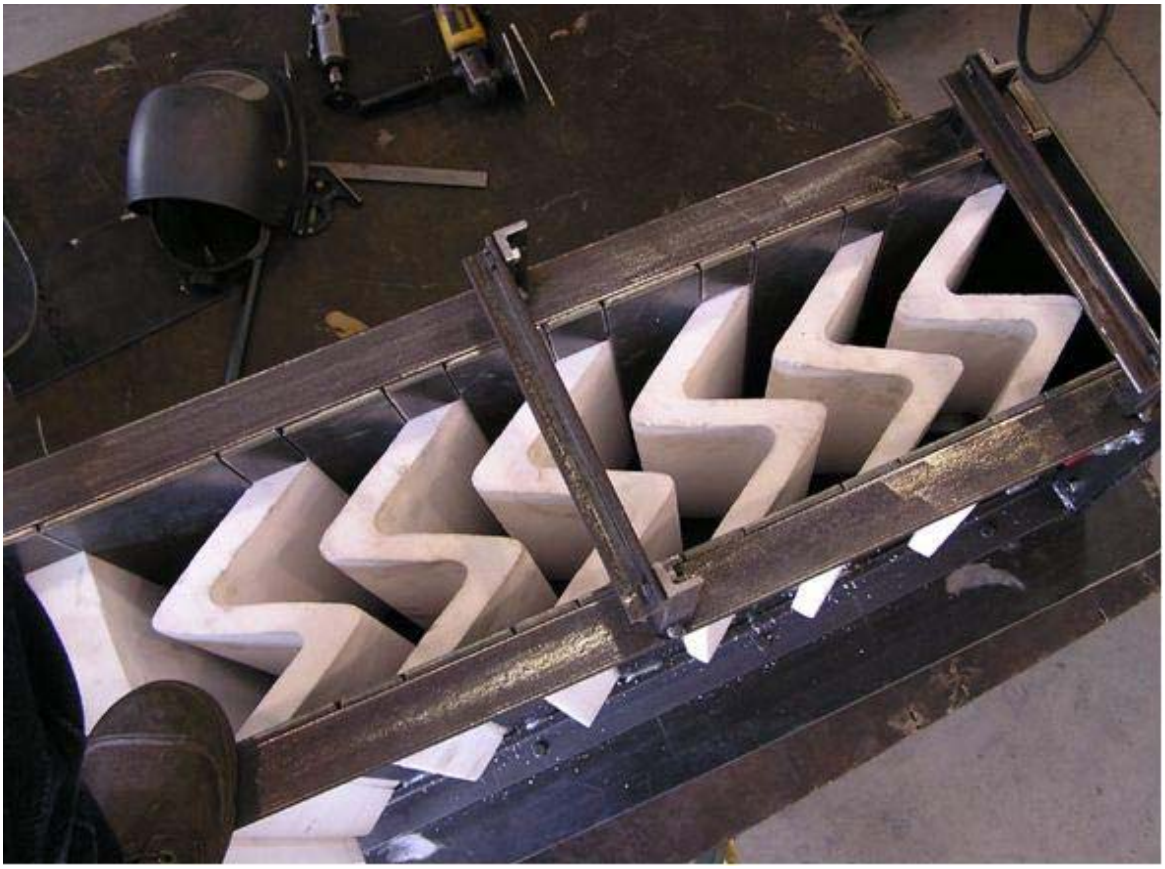

Figure 18: Photograph of the manufactured zigzag channel for insertion in the tundish.

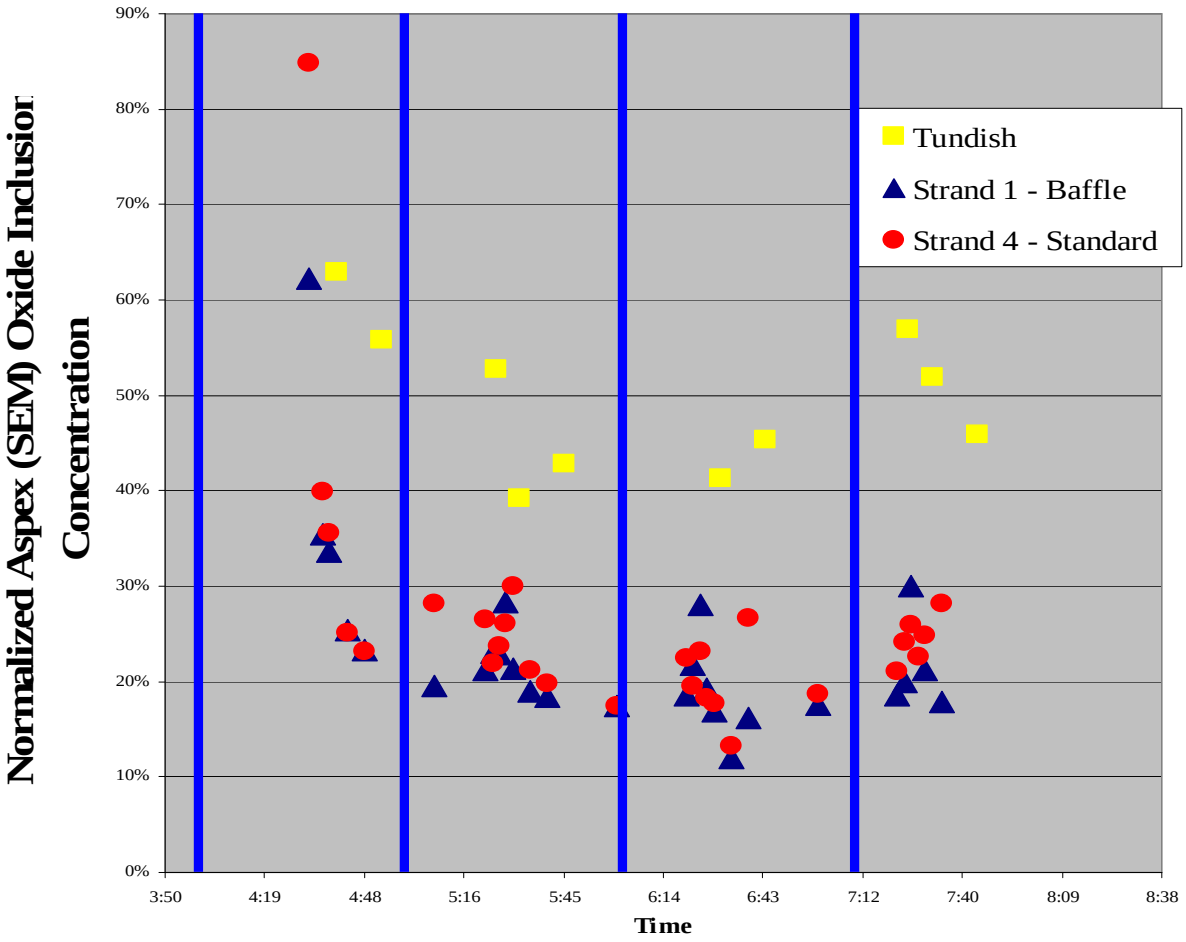

Figure 19: SEM inclusion counts for the steel from the tundish.

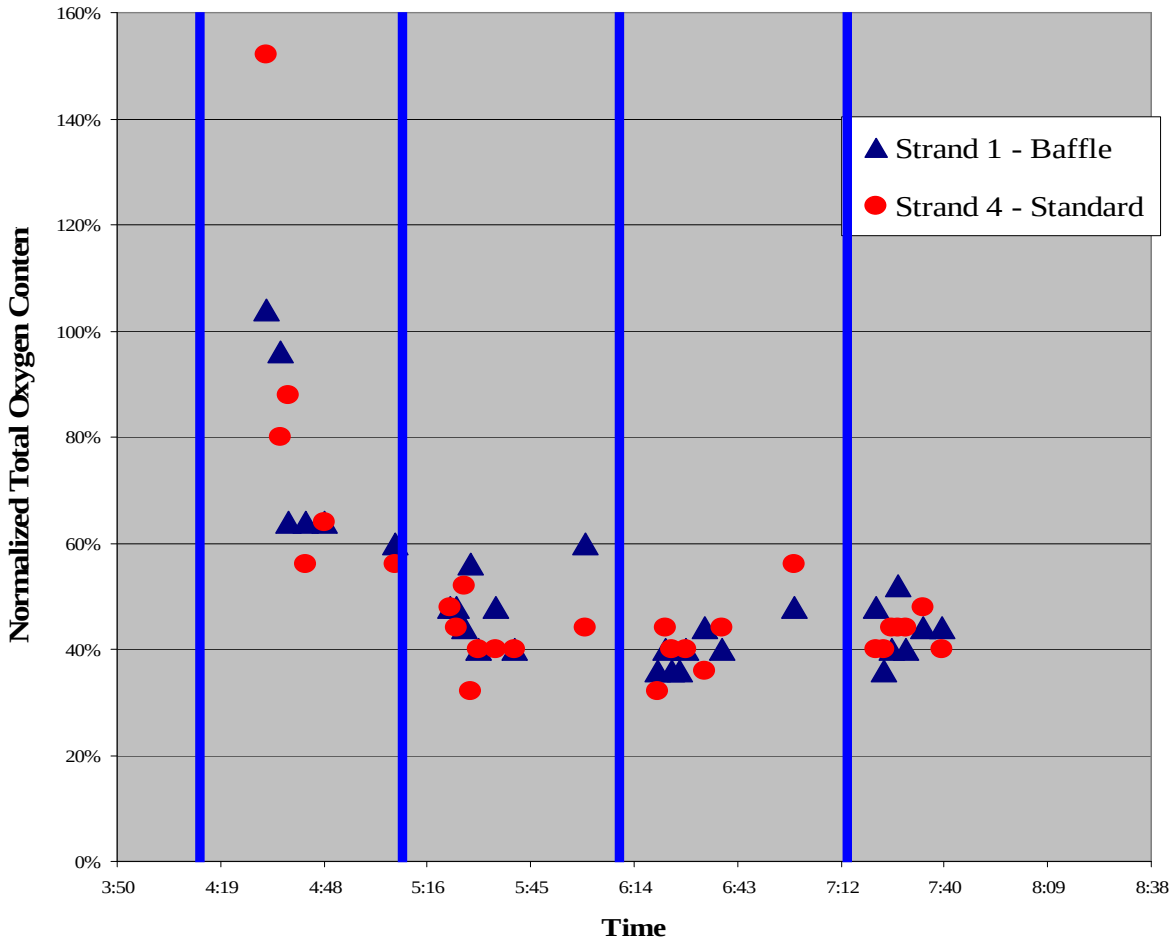

Figure 20: Total oxygen contents of the steel from the baffled and unbaffled strands.

Table 2: Total oxygen contents of the steel from the baffled and unbaffled strands.

Ultrasonic Testing Results

Baffle Trial #2											
		The baffle was put near #1 strand. #4 Strand had no baffles added.									
Grade:	4027										
Strand 1			Strand 4			Strand 1			Strand 4		
Start of tundish			Start of tundish			End of 1st heat			End of 1st Heat		
PartID	Mult L/Vol		PartID	Mult L/Vol		PartID	Mult L/Vol		PartID	Mult L/Vol	
1c1-1	0.1399		4c1-1	0.3498		1c5-1	1.2679		4c5-1	1.6234	
1c1-2	0.8569		4c1-2	0.1341		1c5-2	4.6488		4c5-2	1.8887	
1c1-3	1.2125		4c1-3	0.2536		1c5-3	0.3935		4c5-3	0.0000	
1c1-4	1.7837		4c1-4	0.1282		1c5-4	0.1282		4c5-4	0.3585	
1c1-5	1.5302		4c1-5	0.1370		1c5-5	2.3637		4c5-5	0.0117	
1c1-6	0.8744		4c1-6	2.5357		1c5-6	0.3643		4c5-6	0.0583	
1c1-7	1.4456		4c1-7	0.2157		1c5-7	0.7024		4c5-7	0.0904	
1c1-8	0.5946		4c1-8	0.0874		1c5-8	0.0175		4c5-8	0.0787	
1c1-9	0.3031		4c1-9	0.2507		1c5-9	0.0845		4c5-9	0.0408	
1c1-10	1.6322		4c1-10	1.9091		1c5-10	0.4080		4c5-10	0.0000	
Average	1.0373		Average	0.6001		Average	1.0379		Average	0.4150	
Std Dev	0.5726		Std Dev	0.8711		Std Dev	1.4532		Std Dev	0.7171	
Timken is somewhat confused why the UT results show a degradation of quality on the baffle strand.											
The results may be spurious as they do not agree with total oxygen or SEM results.											

SUMMARY AND CONCLUSIONS

It was attempted to modify the molten steel flow in a continuous casting tundish by introducing into the tundish a baffle that contained specially designed zigzag channels to create turbulence in the flowing molten steel and create a condition where the inclusions within the steel would contact the baffle surface and stick to it removing those inclusions from the steel. The baffle was designed to simulate the conditions that often cause the chemical trapping of inclusions to build up and form accretions at the exit from the SEN into the caster. This research involved recreating the SEN exit conditions by computational fluid dynamic analysis of the flow of the molten steel through the baffle within the tundish. The baffle was built by ANH Refractories to be accommodated within a commercial tundish at Timken. It had a first industrial trial at Timken, for which no evidence of inclusion trapping was evident. In an iteration, a second baffle was then designed with modified channels and subjected to a commercial scale trial as well. Again, there was no evidence of inclusion trapping and no evidence of accretion build up within the baffle channels.

Inclusion contents of the steel from the cast strand with a trapping baffle and a cast strand without the tundish baffle had the same levels of inclusions within the two cast steels. Reducing the size of the baffle channels to increase the level of turbulence of the molten steel passing through the baffle did not reduce the inclusion content below that of the baffle-free casting. The tundish baffle chemical trapping concept was not successful in either of the two industrial trials.

However, with only two trials, one of which was an iteration, it cannot be concluded that the principles upon which the research was based cannot be successful. For example, in industrial practice, not every SEN develops accretions that block the flow of steel into the caster. Perhaps, in the two trials, there just were not situations that would have developed inclusion trapping in the baffle. Neither trial developed accretions in their SENs either. Clearly, many more industrial trials with multiple iterations are needed to fully explore the potential of this inclusion removal process.

There were some positives that resulted from this research effort. From the flow of the molten steel, both in the first trial and then the iteration trial as well, it was evident that the concept of a tundish furniture baffle did not inhibit the flow of the molten steel through the tundish into the SEN and ultimately the caster. This was a major concern to some engineers who were presented the idea. However, this is not assurance that if the baffle channels are accumulating inclusions in the form of accretions, then there would not be any steel flow inhibition. Clearly, the concept of chemically trapping inclusions within a baffle in the tundish in its optimized form would trap inclusions and reduce flow in a manner that would just require baffle replacement at the same time the tundish requires relining. Again, many more iterations would be required for this optimization.

Since there were no accretions developed in the SEN's during each of the two industrial trials, one cannot conclude that the baffle concept is not feasible, only that the concept was not successful during its first two industrial trials, only the second of which had an iterative design.

RECOMMENDATIONS FOR FUTURE RESEARCH

The most obvious recommendation at this time is to create a systematic series of iterations of the baffle design and test them in industrial trials. Two trials, the second of which was an iteration are hardly enough to prove or disprove the principles of the chemical inclusion trapping concept. Perhaps 20 or more industrial trials would be necessary. The only convincing disapproval of the concept would be for the SEN to clog in a system that included a trapping baffle in its tundish.

Much more fluid dynamic modeling is necessary to gain a better understanding of the molten steel flow through the baffle and the tundishes in general. The fact that every tundish is different is not a beneficial feature to the success of this concept. For example, whenever the steel tundish is changed in its size or geometry, the entire modeling of the flow must be repeated. In this research, the multiple changes of industrial trial partners consumed years of tundish re-modeling time.

It is not clear that the "zigzag" concept of the baffle to create turbulence similar to that at the bottom of the SEN is an optimum one, or even one that works or can be successful. That geometry was a first chance guess and most certainly is a point of design improvement. The creation of the turbulence to drive the inclusions against the baffle surfaces where they would chemically bond or adhere and be removed from the molten steel may have better methodologies. Different geometries should be explored in future studies.

The alteration of the surface chemistry of the baffle to promote sticking of the inclusions and enhance their chemical trapping is an unexplored area. Droplet wetting studies could be pursued to better understand the bonding mechanisms that enable the accretions to form in the SEN and then duplicate those surface conditions in the baffle. One obvious thing to try here would be to take accretions from a clogged SEN and then form a surface layer of accretion material within the baffle. Just duplicating the mineralogy of the accretions may not be enough.

It is appropriate to close with noting that the only occasional formation of inclusion accretions in the SEN is indeed a difficult aspect of the' situation. The failure to form accretions or trap inclusions within any baffle design is not a rejection of the concept, unless those same castings form accretions in the SEN.

ACKNOWLEDGEMENT

This work was funded through the American Iron and Steel Institute's Technology Roadmap Program for the Steel Industry (AISI - TRP Project No. 9757) and the US Department of Energy under award DE-FC36-97ID13554. The industrial sponsor is the Timken Company

RESULTING PUBLICATION AND PRESENTATIONS

- Plappally, A.K., Sharif, M.A.R., and Bradt, R.C., "Modeling Molten Steel Flow in a Tundish Equipped with a Spinel Coated Zigzag Channel for Removing Inclusion Particles," *Fluid Dynamics & Materials Processing*, Vol. 3, pp. 115-128, 2007.
- Plappally, A.K., Sharif, M.A.R., and Bradt, R.C., "Removal of Inclusion Particles from Molten Steel in a Tundish with a Spinel Coated Zigzag Channel Insert," Proceedings of the Materials Science and Technology (MS&T) Conference and Exhibition, Cinergy Center, Cincinnati, OH, October 15-19, 2006, The Role of Computational Methods in Materials Research and Development, Organized by V. Tikare, T. Marechaux, D. Apelian, and M. Horstemeyer,: FUNDAMENTALS AND CHARACRERIZATION: Volume 2, pp. 421-432.
- Sharif, M.A.R. and Bradt R.C., "Chemical Trapping of Inclusions from Steel in the Tundish," Proceedings of the St. Louis Refractories Symposium, March 21-22, St. Louis, Missouri, 2002.
- Akbar, M.K., Sharif, M.A.R., and Bradt, R.C., "Effect of Forces on a Particle in a Straight Channel Turbulent Flow," *Proceedings of the 4th International Conference on Multiphase Flow*, Paper No. 947, May 27 – June 1, New Orleans Louisiana, 2001.
- Akbar, M.K., Sharif, M.A.R., and Bradt, R.C., "Turbulent Dispersed Particulate Flow in Zigzag Channel," *Proceedings of the 4th International Conference on Multiphase Flow*, Paper No. 834, May 27 – June 1, New Orleans Louisiana, 2001.
- Akbar, M.K., Sharif, M.A.R., and Bradt, R.C., "Turbulent Dispersed Particulate Flow in a Zigzag Channel," DETC2000/CIE-14675, *Proceedings of the 2000 ASME Design Engineering Technical Conferences*, September 10-13, Baltimore, Maryland, 2000.

REFERENCES

Abhilash, E.; Joseph, M.A.; Krishna, P. (2006): Prediction of dendritic parameters and macro hardness variation in permanent mould casting of Al-12%Si alloys using artificial neural networks. *Fluid Dynamics & Materials Processing*, vol. 2, pp. 211-220.

Amberg, G.; Shiomi, J. (2005): Thermocapillary flow and phase change in some wide spread materials processes. *Fluid Dynamics & Materials Processing*, vol. 1, pp. 81-95.

Chakraborty, S.; Sahai, Y. (1991): Effect of varying ladle stream temperature on the melt flow and heat transfer in continuous casting tundishes. *ISIJ International*, vol. 31, pp. 960-967.

Chevrier, V.F. (2000): Droplet and bubble separation at the interface between a liquid metal and a liquid slag. Ph.D dissertation, Carnegie Mellon University.

Clift, R.; Grace, J.R.; Weber, M.E. (2005): *Bubbles, Drops, and Particles*. Dover Publications.

Dash, K.S.; Jha, K.P. (2002): Effect of outlet positions and various turbulence models on mixing in a single and multi-strand tundish. *International Journal of Numerical Methods for Heat and Fluid Flow*, vol. 12, pp. 560-584.

Dash, K.S.; Jha, K.P. (2004): Employment of different turbulence models to the design of optimum steel flows in a tundish. *International Journal of Numerical Methods for Heat and Fluid Flow*, vol. 14, pp. 953-979.

ESI-CFD (2006): CFD-ACE+^{TM} Manual published by ESI-CFD, Inc.

He, Y.; Sahai, Y. (1990): Influence of some factors on fluid flow in continuous casting tundishes. *Acta Metallurgica Sinica. B*, vol.3. pp. 49-53.

Hong, C.P.; Zhu, M.F.; Lee, S.Y. (2006): Modeling of dendritic growth in alloy solidification with melt convection. *Fluid Dynamics & Materials Processing*, vol. 2, pp. 247-260.

Ichibashi, H. (1986): Application of filter for the clean steel. Proceedings of the Fifth International Iron and Steel Congress, Tundish Metallurgy, vol. 1, pp. 677-687

Ilegbusi, O.J.; Szekely, J. (1987): The modeling of fluid flow, tracer dispersion and inclusion behavior in tundishes. *Mathematical Modeling of Materials Processing Operations*, Szekely, J., eds., TMS, Warrendale, PA, pp. 409-429.

Itoh, H.; Hino, M.; Ban-ya, S. (1997): Thermodynamics on the formation of spinel nonmetallic inclusion in liquid steel. *Metallurgical and Material Transaction B - Process Metallurgy and Materials Processing Science*, vol. 28, pp. 953-956.

Javurak, M.; Kaufmann, B.; Gerhard, Z.; Philipp, G. (2002): Inclusion separation in tundishes - some new general aspects. *Steel Research*, vol. 73, pp. 1-7.

Launder, B.E.; Spalding, D.B. (1974): The numerical computation of turbulent flows. *Computational Methods for Applied Mechanics and Engineering*, vol. 3, pp. 269-289.

Lopez-Ramirez, S.; Morales, R.D.; Serrano, J.A.R. (2000): Numerical simulation of the effects of buoyancy forces and flow control devices on fluid flow and heat transfer phenomena of liquid steel in a tundish. *Numerical Heat Transfer Part A – Applications*, vol. 37, pp. 69-86.

Ludwig, A.; Gruber-Pretzler, M.; Wu, M.; Kuhn, A. Riedle, J. (2005): About the formation of macrosegregations during continuous casting of Sn-Bronze. *Fluid Dynamics & Materials Processing*, vol. 1, pp. 285-300.

Lun, C.K.K.; Liu H.S., (1997): Numerical simulation of dilute turbulent gas-solid flows in horizontal channels. *International Journal of Multiphase Flow*, vol. 23, pp. 575-605.

Nakashima, J.I.; Tanaka, H.; Fukuda, J.; Kiyose, A.; Yamada, W. (2003): Simulation of coagulation of noon metallic inclusions in tundish and their trappings into the solidified shells in continuous casting mould. *Iron Making and Steelmaking*, vol. 30, pp. 151-157.

Patankar, S.V. (1980): *Numerical Heat Transfer and Fluid Flow*. Hemisphere, New York.

Ran, J.; Zhang, L.; Tang, Q.; Xin, M. (2006): Numerical simulation of the particle motion characteristics in boundary layer gas solid rotary flow. *Journal of Fluids Engineering*, vol. 128, pp. 596-601.

Saffman, P.G. (1965): The lift on a small sphere in a slow shear flow. *Journal of Fluid Mechanics*, vol. 22, pp. 385-400. Corrigendum (1968). *Journal of Fluid Mechanics*, vol. 31, pp. 624.

Schwarze, R.; Bbermeier, F.; Janke, D. (2001): Numerical simulation of fluid flow and disperse phase behavior in continuous casting tundishes. Modeling and Simulation in Material Science and Engineering, vol. 9, pp. 297-287.

Shen, F.; Khodadadi, J.M.; Pien, S.J.; Lan, X.K. (1994): Mathematical and Physical modeling studies of molten aluminum flow in a tundish. *Metallurgical and Materials Transaction B - Process Metallurgy and Materials Processing Science*, vol. 25, pp. 669-680.

Sheng, D.Y.; Jonsson, L. (1999): Investigation of transient fluid flow and heat transfer in a continuos casting tundish by numerical anlysis verified with nonisothermal water model experiments. *Metallurgical and Materials Transaction B - Process Metallurgy and Materials Processing Science*, vol. 30, pp. 979-985.

Taniguchi, S.; Brimacombe, J.K. (1997): Application of pinch force to the separation of inclusion particles from liquid steel. *ISIJ International*, vol. 34, pp. 722 -731.

Vargas-Zamora, A.; Morales, R.D.; Diaz-Cruz, M.; Palafox-Ramos, J.; Demedices, L.G. (2003): Heat and mass transfer of a convective-stratified flow in a trough type tundish. International Journal of Heat and Mass Transfer, vol. 46, pp. 3029-3039.